SPATIAL/TEMPORAL INTERDEPENDENCE OF AFTERSHOCKS FOLLOWING THE 10/31/2001 M5.1 ANZA EARTHQUAKE

Final Technical Report for 03HQGR0078

Dr. Frank L. Vernon III

Scripps Institution of Oceanography/IGPP MC 0225
University of California, San Diego
La Jolla, California 92093-0225 USA
Tele: (858) 534-5537 FAX: (858) 534-6354
E-mail: flvernon@ucsd.edu

March 24, 2005

Research supported by the U.S. Geological Survey (USGS), Department of the Interior, under USGS award number 03HQGR0078*. The views and conclusions contained in this document are those of the authors and should not be interpreted as necessarily representing the official policies, either expressed or implied, of the U.S. Government.*

Key Words: Fault Segmentation, Source characteristics, Fault stress interactions

Final Technical Report for 03HQGR0078

Spatial/Temporal Interdependence of Aftershocks following the 10/31/2001 M_L5.1 Anza Earthquake

Dr. Frank L. Vernon III
Scripps Institution of Oceanography/IGPP MC 0225
University of California, San Diego
La Jolla, California 92093-0225 USA
Tele: (858) 534-5537 FAX: (858) 534-6354
E-mail: flvernon@ucsd.edu

Abstract

We study the spatial/temporal behavior of the initial part of the 31 October 2001 M_L 5.1 aftershock sequence in southern California. This sequence occurred directly below the broadband ANZA network, which recorded continuous waveform data at 13 azimuthally well-distributed stations about the study region (nine stations had epicentral distances < 30 km). We have found that the bi-modal distribution of magnitudes (peaks at approximately 0.5 and 1.5) in the aftershock catalog, for events in the Elsinore and San Jacinto fault regions, is an artifact of data sampling. This is due to the fact that small magnitude earthquakes cannot be detected when they are sufficiently distant from the network. When we restrict the data to events directly under the network this bi-modal distribution is significantly diminished. In the initial two hours of this sequence the ANZA catalog contains 608 aftershocks ($0 < M_L < \sim 3.5$), of which the initial five required stations within 30 km for identification. Using a cluster (radius ≤ 1.1km) of 200 representative aftershocks, we track the maximum seismogram amplitude versus earthquake magnitude. This relationship helps us quantify the visibility of aftershocks within the mainshock coda and assess our detection capabilities. Detection of aftershocks is dependant on the source/station distance, the elapsed time, the relative scaling between the mainshock and aftershock magnitudes. We estimate that that for the given source/station geometry, visible aftershocks within the main shock coda include those: (1) over magnitude 3.0 that are within 10 km of the network centroid and 15 seconds or more into the sequence; and (2) over magnitude 2.0 that are within 30 km of the centroid of the network and 80 seconds or more into the sequence. This suggests that any lack of early aftershocks in sequences recorded by sparse networks might reflect inadequate detection capabilities and not a true deficit in early aftershocks.

Non-Technical Abstract

We examine the temporal/spatial behavior of the 10/31/2001 M_L5.1 aftershock sequence in southern California (the distance between the earthquake and the seismic station was < 30 km for nine stations). We have found that the bi-modal distribution of magnitudes (peaks at approximately 0.5 and 1.5) in the ANZA seismic network catalog, for events in the Elsinore and San Jacinto fault regions, is an artifact of data sampling. This is due to the fact that small magnitude earthquakes cannot be detected when they are sufficiently distant from the network. When we restrict the data to events directly under our network this bi-modal distribution is significantly diminished. We find eight detectable aftershocks ($\sim 1.7 < M_L < \sim 3.5$) in the first two minutes of the continuous waveforms from the M_L5.1 aftershock sequence. However, if we were limited to stations >30 km from the mainshock, only 3 of these earthquakes would likely be detected. Identification of aftershocks in the initial part of the sequence depends on the source/station distance, time elapsed since the mainshock, and the relative mainshock and aftershock magnitudes and focal mechanisms. We estimate detectable aftershocks within the mainshock coda include aftershocks that are approximately: (1) over magnitude 3.0 that are within 10 km of the center of the network and 15 seconds or more into the sequences; and (2) over magnitude 2.0 that are within 30 km of the centroid of the network and 80 seconds or more into the sequence. Stations with epicentral distances less than 30 km were required to identify the first 5 cataloged aftershocks in the ANZA sequence. If we were limited to stations greater than 70 km from the mainshock, at least 16 of the initial aftershocks would go undetected

Introduction

On 10/31/2001, a M5.1 earthquake occurred in the middle of the ANZA network that spans the San Jacinto fault zone in Southern California (Figure 1). The ANZA database contains ~3000 aftershocks of this event, complete to M≈0.0. Rarely are continuous aftershock data of such high quality available. These data, in combination with an additional ~37,000 events in the Anza region recorded during the past 20 years by the ANZA seismic network, offer a unique opportunity to study earthquake processes. In particular we focus on the magnitude distribution of the data, the spatial distribution of the aftershocks and the temporal behavior of the initial part of the sequence.

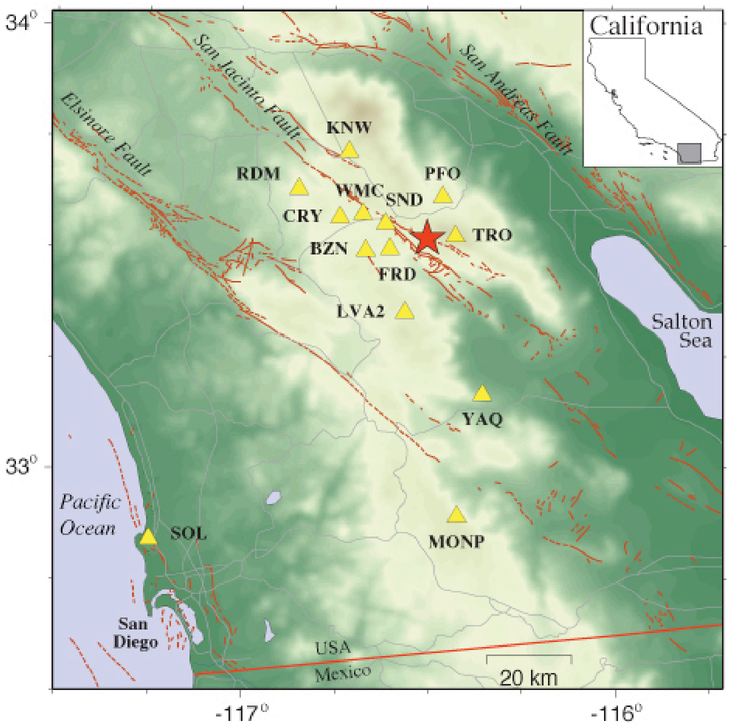

Figure 1. *The location of the 10/31/2001 ANZA M_L5.1 mainshock earthquake (star) in southern California, and its spatial relationship with the ANZA seismic network stations (triangles). Nine stations are within 30 km of the mainshock event.*

The M_L 5.1 ANZA sequence

The 31 October 2001 Anza M_L 5.1 earthquake (33.52°; -116.50°; depth 18 km) occurred directly under the ANZA seismic network, which spans the San Jacinto fault zone in southern California (http://eqinfo.ucsd.edu/deployments/anza.html). Of the 13 24-bit broadband ANZA network stations that recorded the ANZA earthquake, eight were within 20 km of the epicenter (see Figure 1). From 8969 analyst picked seismic wave arrivals, we identified 608 earthquakes in the initial two hours of the Anza M_L 5.1 sequence. Ten or more ANZA three-component broadband stations recorded 527 of these initial 608 aftershocks. This initial two-hour aftershock catalog is complete to M_L≈0.3 and 88% of the aftershocks (534) have magnitudes of 1.0 or below.

Availability of seismic data

We have a world-wide-web home-page for the ANZA network, http://eqinfo.ucsd.edu, which provides maps and information about our database, stations, hardware configurations, including all network metadata in dataless seed volumes. We compile special event web pages (http://eqinfo.ucsd.edu/special_events/index.html) for significant local, regional, and teleseismic events and maintain our *dbrecenteqs* webpages showing the latest seismicity on local, regional, and global scales (*e.g.*, http://eqinfo.ucsd.edu/dbrecenteqs/anza/AZ_R2_map.html). The complete waveform data set of the ANZA network data, which consists of over ~59,000 events, is stored on-line on a RAID mass storage. These data are stored in the standard CSS 3.0 format complete with instrument responses and they are accessible over the Internet. A data request is satisfied by placing the data in a directory for retrieval via the Internet or by sending a tape copy. Additional information can be obtained by sending email to anzanet@epicenter.ucsd.edu. At present we provide data in the following formats: CSS 3.0, SAC, or SEED. The IRIS Data Management Center is maintaining a complete copy of our data archive (updated in real-time) and ANZA data is integrated into their standard FARM database and BUD real-time data distributions. Researchers from academia and industry have complete access to all ANZA data and results directly through UCSD or can access data through the SCEC Datacenter or the IRIS DMC.

Results Part #1: The Apparent Bi-Modal Distribution Of Earthquake Magnitudes.

We have found that the bi-modal distribution of magnitudes (peaks at approximately 0.5 and 1.5) in the ANZA seismic network catalog, for events in the Elsinore and San Jacinto fault regions, is likely an artifact of data sampling. This is due to the fact that small magnitude earthquakes cannot be detected when they are sufficiently distant from the network. When we restrict the data to events directly under our network this bi-modal distribution is significantly diminished.

Results Part #2: The Spatial Distribution Of Aftershocks In The 31 October 2001 M_L 5.1 ANZA Aftershock Sequence.

A striking feature of the aftershock distribution of the M_L 5.1 event is a void of seismicity that forms an ‘X’ pattern (Figure 2). This peculiar absence of seismicity forms a primary band that trends ~N45°W, an orientation similar to the San Jacinto fault (see Figure 1). We investigated simple causes of this seismicity void and we were able to eliminate the following causes from contention: Auto-generation of the locations (all events reviewed by an analyst); different analysts processing the data (Dr. Martynov Processed ~85% of the data, and we found no systematic relationship between the six analyst who processed these data and the aftershock locations); round off problem in the latitude and longitude locations; the result of four separate sequences.

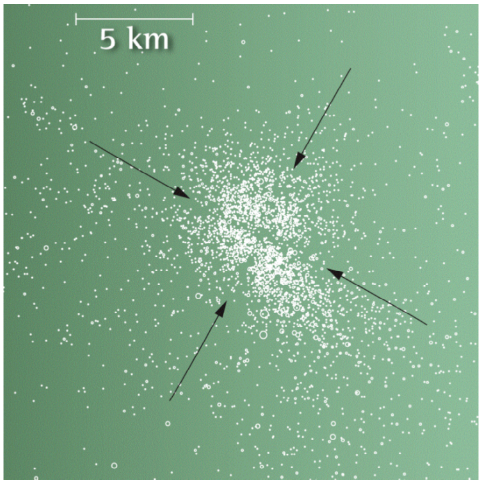

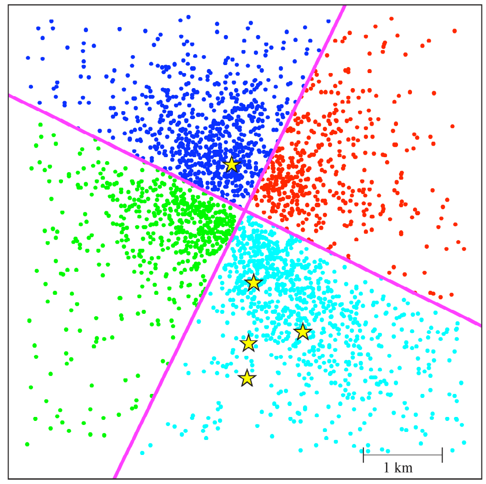

Figure 2. *(Left) A void forming an "X" is found in the seismicity distribution of the M_L 5.1 ANZA aftershock sequence. (Right) Dividing the data into the four quadrants defined by the void, the larger earthquakes (M_L>2, indicated by stars) are found in only the NW and SE quadrants.*

Many studies examine the correlation between mainshock generated stress changes and aftershock locations and assume correlation implies causality. We apply this technique to our data set. We compute static stress changes from a mainshock event using the boundary element computer program 3ddef (http://www.ceri.memphis.edu/~ellis/3ddef/index.html). Our mainshock geometry is a vertical right-lateral strike-slip fault, striking at 296 degrees, which is consistent with the 31 October 2001 ANZA M_L 5.1 mainshock. We derive stress changes on aftershocks similarly oriented throughout our ~6 km by 6 km study region, derived at uniformly spaced grid nodes separated by 50 meters at a depth of 14.5 km. The stress changes we consider include: Coulomb stress, shear stress, normal stress and pressure. Because the northwest (NW) and southeast (SE) quadrants tend to have slightly more events than the other quadrants, and because they also contain the only earthquakes over magnitude two, we look for stress patterns that have more pronounced stress increases in the NW and SE quadrants. Qualitatively, out of all the stress changes tested, the normal stress changes best predict the largest encouragement of aftershocks in the NW/SE quadrants (Figure 3). We caution that these stress change calculations are very sensitive to the orientation and slip direction of both the mainshock and the individual aftershocks. Changes as small as 30 degrees can drastically alter the stress patterns and in turn the correlation with the aftershocks. Because we do not have a full aftershock focal mechanisms catalog we are unable to assess if they strongly mimic the mainshock mechanism. In fact, the small correlation in waveforms from nearby aftershocks indicates that the aftershock focal mechanisms might be very diverse (Figure 4). We can therefore conclude that a correlation is possible but not conclusive. Additional analyses of the aftershock fault orientations are required to obtain more robust results.

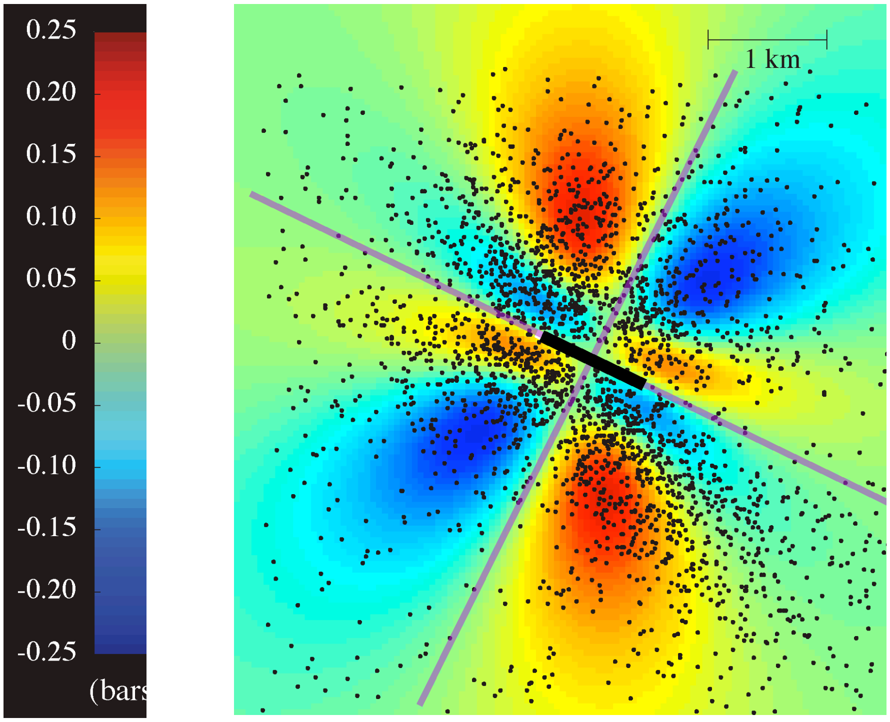

Figure 3. *Normal stress changes generated by a mainshock event with: strike=296 degrees, dip = 90 degrees, and rake = right lateral. The aftershock fault orientations are assumed to be similarly oriented. We caution that if these fault orientations and direction of slip are altered by as little as 30 degrees this pattern of stress increases (red) and stress decreases (blue) can be drastically changed.*

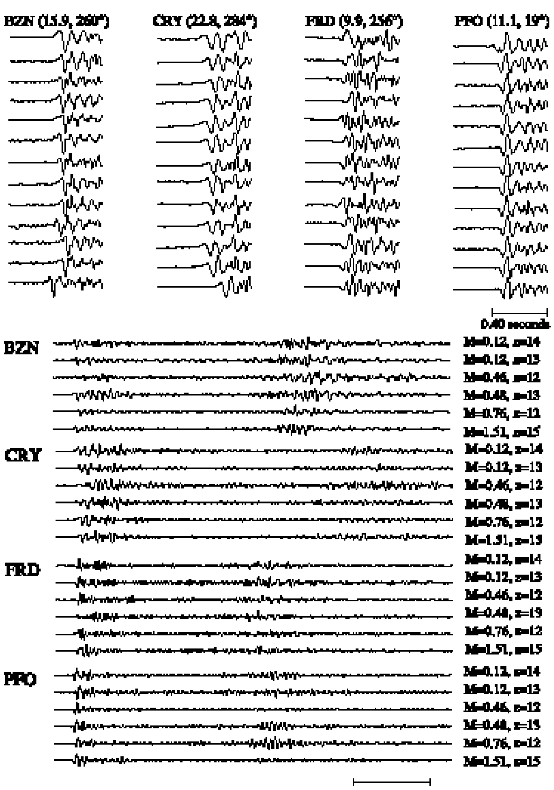

Figure 4. *Waveforms of select aftershocks of the M_L5.1 10/31/2001 earthquake. (top) Similar waveforms are found in some regions (station code, distance in km, and azimuth are indicated), but (bottom) this is not always the case as seen in a cluster of aftershocks within ±2km of the mainshock (station code, depth, and magnitude indicated). All traces are normalized to unit amplitude.*

Results Part #3: The Temporal Behavior Of Aftershocks In The Initial Portion Of The M_L5.1 Earthquake Sequence

It is difficult to identify aftershocks in the initial part of an aftershock sequence for a number of reasons including aftershocks obscured in the coda of the mainshock, errors in unraveling seismic waveforms of temporally overprinted events, minimal signal to noise ratios for small events, events with large source/station distances and/or limited recording bandwidth. These difficulties often make it impossible to identify clearly the onset of the aftershock sequence. To more easily identify aftershocks in the initial part of the ANZA aftershock sequence we use a high pass filter to help identify seismic arrival times of the aftershocks and in turn determine the aftershock locations. In this way, we cataloged 608 events ($0<M_L<\sim3.5$) in the initial two hours of this sequence. For these events the mean time between consecutive aftershocks is ~12 seconds (Figure 5). This lag time of ~12 seconds is not dictated by the coda of the first earthquake obscuring the next earthquake's signal, as the duration of the coda of most of the aftershocks is typically only ~1 second.

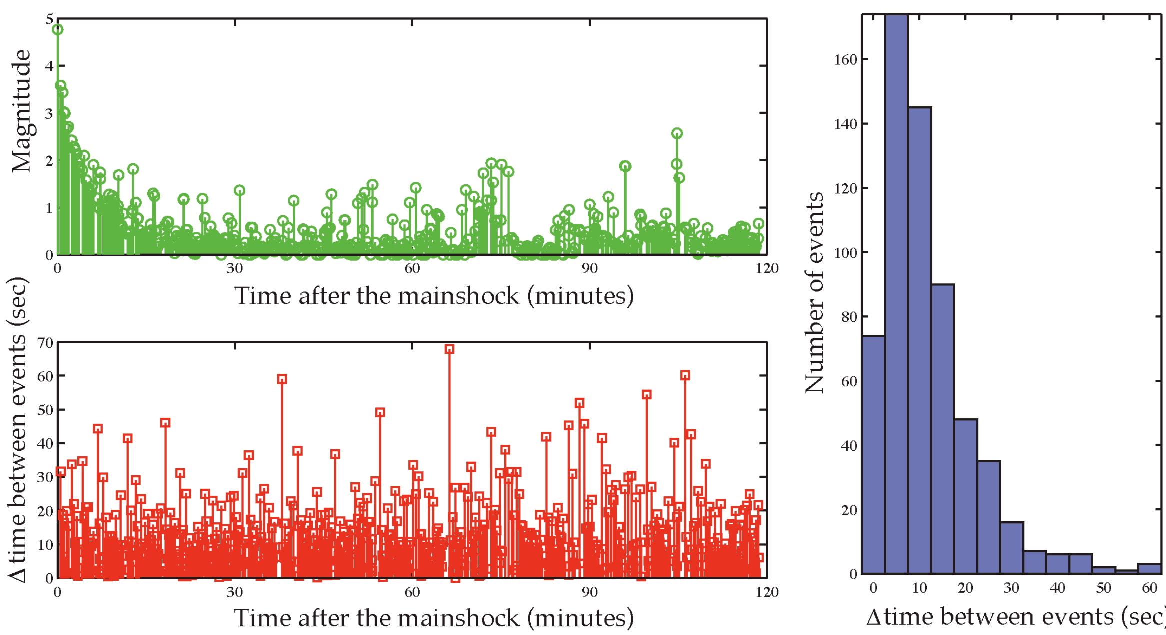

Figure 5. *Temporal behavior of the first 608 aftershocks in the ANZA M_L5.1 sequence. In the first two hours of the sequence the mean time between successive aftershocks is ~7 seconds.*

Earthquakes can go undetected when there is sparse network coverage and when the signal-to-noise-ratio (SNR) is small. To establish additional methods to help identify missed aftershocks, we compute the envelope of the mainshock seismograms (computed using a Hilbert transformation) and we smooth these envelopes using a centered 50-point moving average (equivalent to a 0.5 second time window). Using these envelopes, we can more easily identify increases within the mainshock coda and correlations of these increases across the network, which may indicate an overprinted aftershock. In this way, we identified increases in the amplitude of these envelopes at ~110 seconds, ~150 seconds, and ~175 seconds into the sequence, which correspond to earthquakes of magnitude 2.2, 2.13 and 1.72, respectively. These aftershocks, however, were already found in the initial processing of the continuous ANZA waveform data.

Correlation of seismic signals across multiple stations can aid in the identification of aftershocks, especially for small magnitude aftershocks obscured by the mainshock's large coda. This was the case for the first aftershock we found at ~15 seconds into the ANZA sequence. This aftershock was identified at stations TRO (epicentral distance 6.7 km) and PFO (epicentral distance 11.5 km). The second identifiable aftershock occurred 31.6 seconds into the sequence and was observed at ANZA stations TRO, PFO, and FRD (epicentral distance 11.0 km). The magnitudes of these initial two aftershocks are difficult to determine because they are overprinted in the coda of the mainshock but, as discussed below, we estimate that both events were above magnitude 2.7. In the automated detection of the broadband data no aftershock is identified in the first ~2 minutes of the sequence (Figure 6). However, careful analyses of the waveform data (both seismograms and spectrograms) allowed us to identify additional aftershock in the first two minutes of the continuous waveforms (Table 1).

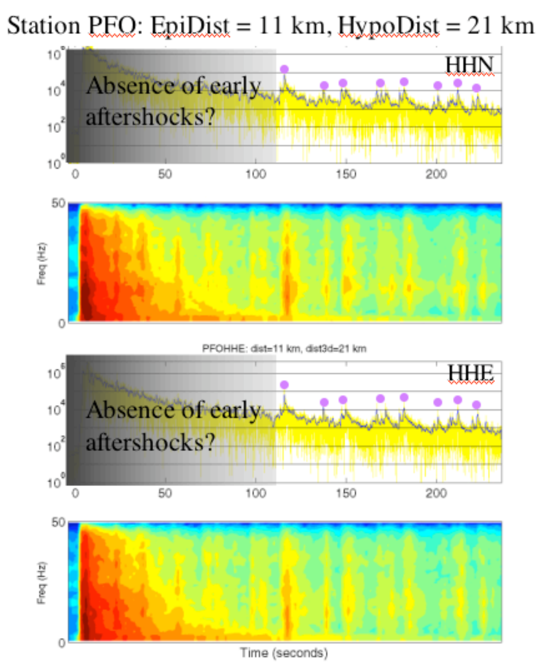

Figure 6. *Both frequency and amplitude information can be used in identifying early aftershocks. For example, at station PFO the amplitude information alone shows obvious increases (indicated with purple dots), which likely correspond to aftershocks, only after ~2 minutes or more into the sequence. However, vertical bands of higher frequency energy in the spectrograms indicate aftershocks do occur in the earlier part of the sequence (i.e., at ~30 and ~65 seconds).*

In general, identification of one earthquake within the coda of a previous earthquake requires that the amplitude of the second event exceed the deviations, or fluctuations, within the first earthquake's coda. When the first event is smaller than the second, typically both can easily be identified even if there is a relatively small time separation between the two earthquakes. For example, at station FRD, a magnitude 1.1 earthquake (the maximum absolute seismic amplitude, Δamp, is ~1,700 counts) that occurred ~0.4 seconds before a magnitude 2.6 earthquake (Δamp ~59,000 counts) is easily identified (Figure 7). When the first event is much larger than the second, as is the case for mainshocks and their initial aftershocks, overprinting is particularly problematic because the large mainshock signal obscures the smaller aftershocks.

To quantify our aftershock detection capabilities we first establish, at each station, the relationship between the magnitude of each aftershock and the maximum amplitude (Δamp) of the associated seismogram. To avoid Δamp measurements being strongly influenced by the depth of the earthquake or variability in source/station distance, we limit our data to a tight cluster of 200 aftershocks (cluster radius < 1.1 km; ~0.0 < M_L < 2.7, (cluster centroid of -116.50°, 33.52°, 16.4 km; cluster radius < 1.1 km)). We eliminate non-seismic long period signals (*e.g.*, microseisms) by applying a 1 Hz high-pass Butterworth filter to the continuous waveform data before processing. As expected, the stations closest to the source area have seismograms with larger amplitudes and, in general, the amplitudes diminish with aftershock magnitude (Figure 8).

We next determine what magnitude aftershocks should be visible within the mainshock coda. We assume that an aftershock is identifiable if its maximum absolute seismic amplitude is on par with the amplitude deviations within the mainshock coda. To quantify the mainshock amplitude fluctuations, we determine the maximum absolute amplitude of the peak-to-peak signal within a ±0.25 second window (50 data points for these 100sps data) for each time step within the first two minutes of the sequence. In this way we obtain an estimate of the fluctuation of the mainshock coda as a function of time. Using these measurements and the previously established amplitude/magnitude relationship (see Figure 8), we can quantify our detection capabilities (Table 1). We estimate that that for the given source/station geometry, visible aftershocks within the mainshock coda include those: (1) over magnitude 3.0 that are within 10 km of the network centroid and 15 seconds or more into the sequence; and (2) over magnitude 2.0 that are within 30 km of the centroid of the network and 80 seconds or more into the sequence.

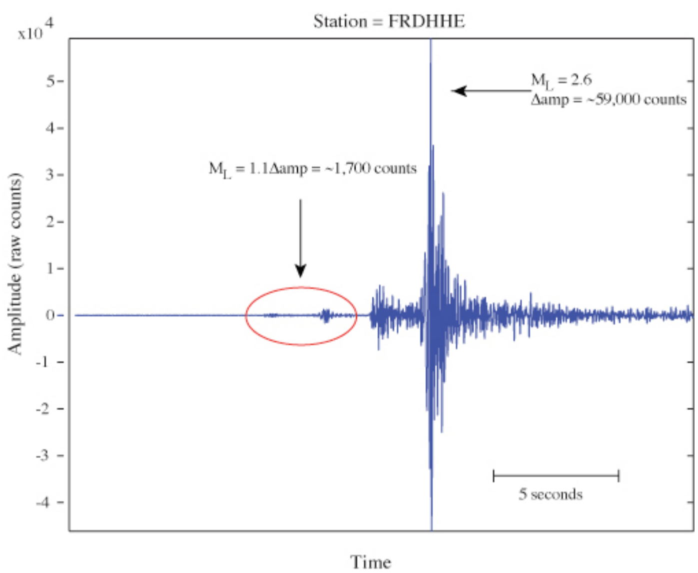

Figure 7. *Seismic recording at ANZA station FRD of two earthquakes: a magnitude 1.1 earthquake followed almost immediately by a magnitude 2.6 earthquake. If the magnitude 1.1 event instead occurred in the coda of the 2.6 event, its signal would be obscured and detecting it would be challenging.*

When identifying early aftershocks, there is a trade-off between the benefits of the larger amplitude signal at the near-source recordings (*e.g.*, station TRO) and the obscuring of these signals by the large mainshock signal. Aftershock detection is also dependent on the mainshock and aftershock focal mechanisms. In situations where the mainshock coda falls off relatively rapidly (*e.g.*, station FRD), it is more likely that aftershock signals can be identified. Here, we find that stations with epicentral distances less than 30 km were required to identify the first five cataloged aftershocks in the ANZA sequence. If we were limited to stations greater than 70 km from the mainshock, at least 16 of the initial aftershocks would go undetected (Figure 10).

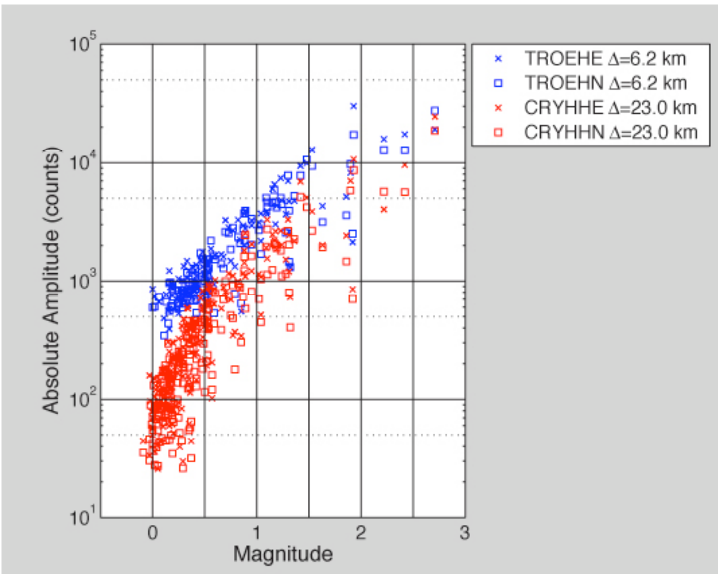

Figure 8. *Quantifying the maximum amplitude (in counts) of broadband recordings of seismic waves (primarily dominated by the S-wave) as a function of earthquake magnitude. Data shown is limited to a tight cluster of 200 earthquakes. Presented are the results from stations TRO and CRY. (Epicentral distances, Δ, are listed, see Figure 1 for station locations.)*

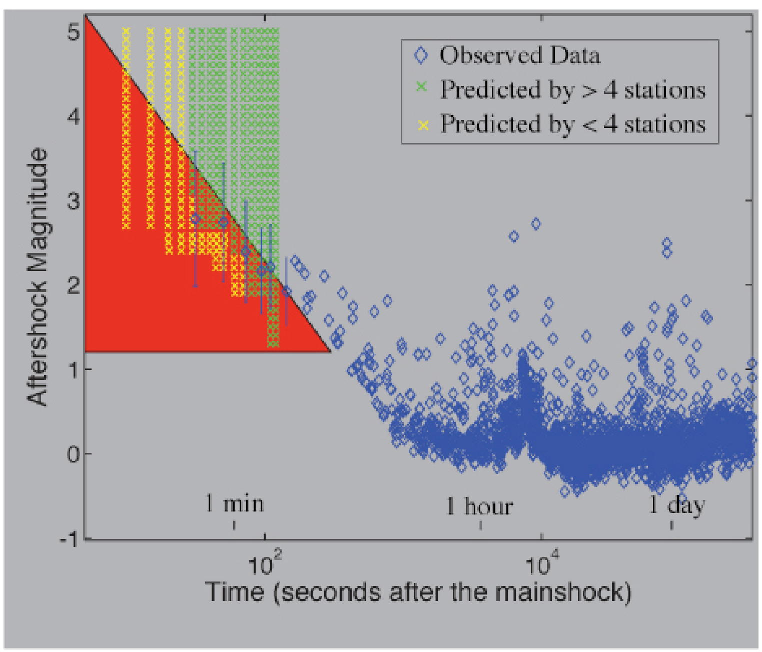

Figure 9. *The 31 Oct 2001 aftershock sequence. The magnitudes of the initial six aftershocks we identified in the sequence have large uncertainties (shown with error bars) because the signals are overprinted in the coda of the mainshock making these signals difficult to separate.*

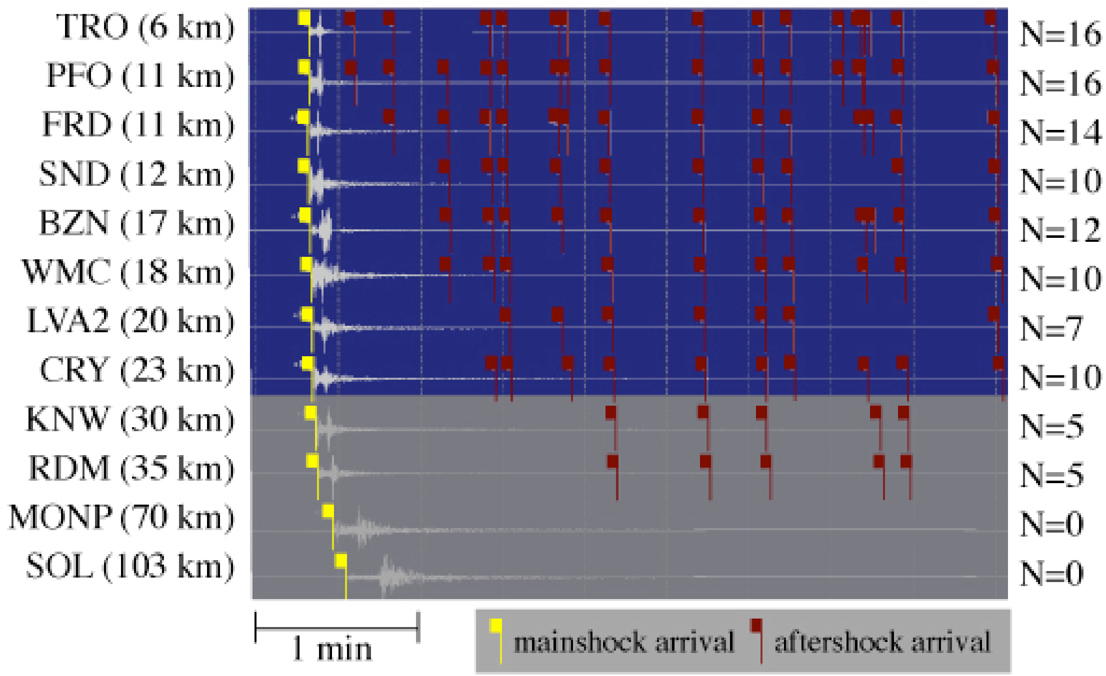

Figure 10. *Temporal behavior of the 31 October, 2001 Anza M_L 5.1 aftershock sequence. The station name and epicentral distance is listed on the right-hand side, and the number of aftershocks (N) listed on the left-hand side. Stations with epicentral distances less than 30 km are required to identify the first 8 aftershocks in the sequence. Without these stations, these events would not be cataloged. At the more distant stations (>70 km), the initial 16 events in our catalog are not detectable.*

Table 1. *Identification of the first observable aftershocks in the M_L5.1 ANZA aftershock sequence (Yes = detectable; -- = not detectable). Also listed are the elapsed times between the mainshock and aftershock of interest (Δt) and the elapsed time between subsequent earthquakes (Δlag).*

Station	Epi-Distance (km)	Hypo-Distance (km)	**Main-shock**	Earth-quake #1	Earth-quake #2	Earth-quake #3	Earth-quake #4	Earth-quake #5	Earth-quake #6	Earth-quake #7	Earth-quake #8
M_L			***5.1***	< 3.5	~2.6	~2.4	~2.0	~1.9	~1.9	~1.7	~2.2
Δt (sec)			***0.0***	15.0	31.6	50.3	66.6	73	93	94.5	110.
Δlag (sec)			***0.0***	15.0	16.6	18.7	16.3	6.4	19.9	1.6	15.5
TRO	6.206	16.601	YES	YES	YES	N/A	YES	YES	YES	YES	YES
PFO	10.523	18.650	YES	YES	YES	YES	YES	YES	YES	YES	YES
FRD	10.580	18.682	YES	--	YES	YES	YES	YES	YES	YES	YES
SND	11.661	19.315	YES	--	--	YES	YES	YES	YES	YES	YES
BZN	16.504	22.571	YES	--	--	YES	YES	YES	YES	YES	YES
WMC	17.853	23.576	YES	--	--	YES	YES	YES	YES	YES	YES
LVA2	19.913	25.172	YES	--	--	--	YES	YES	YES	YES	YES
CRY	23.205	27.848	YES	--	--	--	YES	YES	YES	YES	YES
KNW	29.537	33.310	YES	--	--	--	--	--	YES	YES	YES
RDM	35.060	38.292	YES	--	--	--	--	--	YES	YES	YES
MONP	70.190	71.859	YES	--	--	--	--	--	--	--	--
THSB	98.845	100.037	YES	--	--	--	--	--	--	--	--
SOL	103.260	104.402	YES	--	--	--	--	--	--	--	--

Conclusions

The M_L 5.1 (10/31/2001) ANZA earthquake sequence gave us the unique opportunity to record a sizable earthquake (M_L>5) on a broadband network that was azimuthally well distributed about the study region and near to the earthquake source (*i.e.,* nine stations are within 30 km from the mainshock). Using these continuous data, we investigate the temporal behavior of the initial part of the aftershock sequence. In agreement with previous results, we find that with careful plotting and filtering techniques, 'missed aftershocks' (*i.e.,* those not identified by routine processing) can be identified within the mainshock coda (*e.g.,* Vidale *et al.,* 2003). We have found that the bi-modal distribution of magnitudes (peaks at approximately 0.5 and 1.5) in the aftershock catalog, for events in the Elsinore and San Jacinto fault regions, is an artifact of data sampling. This is due to the fact that small magnitude earthquakes cannot be detected when they are sufficiently distant from the network.

Here, we have shown that detection of early aftershocks depends on: (1) Source/station distance and overall source/station geometry (*i.e.,* sufficient azimuthal coverage); (2) Number of seismic stations (*i.e.,* correlation across multiple stations helps in earthquake identification); (3) The magnitude and magnitude difference between the mainshock and aftershocks; (4) The elapsed time between the mainshock and aftershocks and the elapsed time between consecutive aftershocks; (5) The mainshock/aftershock focal mechanisms and depths; and (6) The recording bandwidth.

We find eight detectable aftershocks ($\sim 1.7 < M_L < \sim 3.5$) in the first two minutes of the continuous waveform data. If we were limited to stations greater than 30 km from the mainshock, only three of these first eight aftershocks would likely be detected; if the stations were limited to those 70 km or greater from the mainshock, none of the first 16 aftershocks would have been identified. We estimate detectable aftershocks within the mainshock coda includes aftershocks that are approximately: (1) over magnitude 3.0 that are within 10 km of the network centriod and 15 seconds or more into the sequences; and (2) over magnitude 2.0 that are within 30 km of the centroid of the network and 80 seconds or more into the sequence. Our results suggest that any lack of seismicity in the initial part of aftershock sequences may be merely a result of limitations of the detection capabilities and not a true phenomenon. For the well recorded ANZA sequence we expect aftershocks $M_L > 2.7$ should detectable after 20 seconds. For sequences recorded by sparse networks and/or when no near-field recordings are available (e.g., closest station > 30km) any absence of ‘early’ aftershocks could be a detection problem and not a true phenomenon.

Bibliography

Kilb, D., V.G. Martynov and F. L. Vernon, Examination of the Temporal Lag Between the 31 October 2001 Anza, California, M_L 5.1 Mainshock and the First Aftershocks Recorded by the Anza Seismic Network, Manuscript in preparation, 2005.

Kilb, D., Martynov, V., and F. Vernon, Examination of the Temporal Lag Between the 31 October 2001 Anza, California, M 5.1 Mainshock and the First Aftershocks Recorded by the Anza Seismic Network. SSA abstract 04-149, G6, 2004.

Vernon, F. *et al.,* Review of ANZA Seismic network, Research and Unanticipated Directions, J. Brune Symposium, Reno, NV, November, 2004.

Kilb, D., V. Martynov, F.L. Vernon, Spatial/Temporal interdependence of aftershocks following the 10/31/2001 M5.1 Anza Earthquake, AGU abstract, 2004.

SF 269, Financial Status Report

FINANCIAL STATUS REPORT
(Short Form)
(Follow instructions on the back)

1. Federal Agency and Organizational Element to Which Report is Submitted U.S. GEOLOGICAL SURVEY	2. Federal Grant or Other Identifying Number Assigned By Federal Agency 03HQGR0078 Vernon	OMB Approved No. 0348-0039

3. Recipient Organization (Name and complete address, including ZIP code)
University of California, San Diego
Post Award Financial Services, 0954
La Jolla, CA 92093-0954

4. Employer Identification Number 956006144	5. Recipient Account Number or Identifying Number 22674A	6. Final Report [X] Yes [ ] No	7. Basis [✓] CASH [ ] ACCRUAL
8. Funding/Grant Period (see instructions) From: (Month, Day, Year) 6/1/03	To: (Month, Day, Year) 12/31/04	9. Period Covered by this Report From: (Month, Day, Year) 6/1/03	To: (Month, Day, Year) 12/31/04

10. Transactions:	I Previously Reported	II This Period	III Cumulative
a. Total outlays	0.00	44,379.41	44,379.41
b. Recipient share of outlays	0.00	0.00	0.00
c. Federal share of outlays	0.00	44,379.41	44,379.41
d. Total unliquidated obligations			0.00
e. Recipient share of unliquidated obligations			0.00
f. Federal share of unliquidated obligations			0.00
g. Total Federal share (Sum of lines c and f)			44,379.41
h. Total Federal funds authorized for this funding period			44,644.00
i. Unobligated balance of Federal Funds (Line h minus line g)			(264.59)

11 INDIRECT EXPENSE				
a. Type of rate:	[ ] PROVISIONAL	[✓] PREDETERMINED	[ ] FINAL	[ ] FIXED
b. Rate 52.0%	c. Base 29,196.99	d. Total Amount 15,182.43	e. Federal share 15,182.42	

12. Remarks: *Attach any explanations deemed necessary or information required by Federal sponsoring agency in compliance with governing legislation*

Report Contact: Teresa G Ornelas (858) 534-0769

13. Certification: I certify ot the best of my knowledge and belief that this report is correct and complete and that all outlays and unliquidated obligations are for the purposes set forth in the award documents.

Typed or Printed Name and Title for Dan M. Gilbreath, Director Post Award Financial Services	Telephone (Area code, number and extension) (858) 534-0769
Signature of Authorized Certifying Official Marian V. Ortiz	Date Report Submitted 1/6/05

NSN 7540-01-218-4387 269-201 Standard Form 269A (REV 4-88)
Prescribed by OMB Circulars A-102 and A-110